Novel Ultrafast Transient Hot-Bridge Technique for Thermal Properties Measurement of Dielectric Thin Films

Boubakeur Essedik Belkerk, Amine Achour, Bertrand Garnier, Mohamed-Abdou Djouadi

Novel Ultrafast Transient Hot-Bridge Technique for Thermal Properties Measurement of Dielectric Thin Films

Boubakeur Essedik Belkerk, Amine Achour, Bertrand Garnier and Mohamed-Abdou Djouadi

***Abstract*—This paper introduces an ultrafast transient hot-bridge technique for the microscale measurement of thermal properties. The system comprises microfabricated heaters and resistance thermometers, arranged in a Wheatstone bridge configuration, deposited on sample surface. These components are used in order to generate and detect electrical pulses, leading to temperature increases on micro- and nanosecond scales. The design and performance of various probes are discussed, with an evaluation of their capabilities in terms of time response, precision and resolution. Electrical pulses are applied via metalized probes, and the resultant temperature increases are analyzed within selected time periods ranging from 10 ns to 100 µs. By ensuring a self-balanced condition for all Wheatstone bridges, the technique facilitates the detection of rapid, time-dependent changes in thermal properties due to temperature evolution or structural transformations. This innovative method enables the measurement of thermal conductivity in very thin films and demonstrates the potential for measuring thermal properties at micrometric or even nanometric scales.**

***Index Terms*—Aluminum nitride, nano-scale and micro-scale thermal transport properties, sapphire, thermal conductivity, thin films, transient hot-bridge, Wheatstone bridge.**

I. INTRODUCTION

Thermal transport properties at the microscale play a crucial role, especially in the thermal management of electronic and electro-optical devices. The thermal properties of thin films can significantly differ from those of bulk materials due to reduced phonon scattering, which is influenced by lattice imperfections and boundaries, primarily at small thicknesses[1,2]. Consequently, measuring the thermal properties becomes a critical step for various applications[3-5]. Numerous techniques are available for measuring thermal transport properties at the microscale and even nanoscale, among which the 3ω method [6-8] and the thermo-reflectance method [9-11] are frequently utilized. However, many of these methods entail complex measurement procedures that could affect the estimation of thermal properties in thin film materials. Furthermore, the complexity

Boubakeur Essedik Belkerk is with the *Universités de Constantine, Laboratoire Microsystèmes et Instrumentation (LMI), Université Constantine 1, Faculté des Sciences de la Technologie, Route de Ain El Bey,* Constantine 25017, Algeria (e-mail: boubakeur.belkerk@gmail.com).
Amine Achour is with the Pixium Vision S.A. 74 Rue du FGB Saint-Antoine, 75012 Paris, France (e-mail: a_aminph@yahoo.fr).
Bertrand Garnier is with the Laboratoire de Thermique et Énergie de Nantes (LTeN) CNRS Nantes Université, La Chantrerie rue Christian Pauc BP 90604, 44306 Nantes Cedex 3. (e-mail: bertrand.garnier@univ-nantes.fr).
Mohamed-Abdou Djouadi is with the Institut des Matériaux Jean Rouxel (IMN), Nantes Université, 2 rue de la Houssinière BP 32229, 44322 Nantes cedex 3, France (e-mail: Abdou.Djouadi@cnrs-imn.fr).

of mathematical analysis and the sophisticated equipment required for measuring thermal properties lead to significant drawbacks [12]. Therefore, new techniques for measuring the thermal properties of thin film materials are required, underscoring the context and importance of our work.

In the current study, we introduce a novel approach that uses ultrafast Transient Hot-Bridges (THB) with electrical heating. This method is inspired by the transient hot wire technique [13] and the transient hot strip technique [14-16], which are widely used for determining the thermal transport properties of solids, liquids and gases [17,18]. The THB technique was originally proposed and developed by Hammerschmidt and coworkers [19,20] for measuring the thermal properties of liquids and bulk materials.

The unique aspect of our technique lies in the use of ultra-fast pulsed excitation, enabling the exploration of transient temperature events within a short time interval ranging from 10-8 to 10-4 seconds. The THB method aims to access to thermal properties on measuring temperature variations induced by ultra-short electrical pulses applied through metalized probes patterned on the material under test. We propose a new probe configuration for measuring the thermal properties of thin films. The design and performance of these probes are optimized and validated theoretically through Comsol Multiphysics finite element modeling (FEM) simulations. Furthermore, we have demonstrated the efficacy of our probes in experimental measurements of thermal properties at various temperatures. Preliminary results were obtained for a 1200 nm-thick silicon oxide (SiO_2) film deposited on a silicon substrate. The technique performance is demonstrated on other materials covering a large thermal conductivity range, such as crystallized bulk-sapphire and aluminum nitride (AlN) thin film.

II. EXPERIMENTAL SECTION

The typical geometry of the sample for Ultra-fast THB measurement is depicted in Figure 1. Such configuration comprises four rectangular metal strips, each with equal electrical resistances but of different sizes, arranged in a Wheatstone bridge. An inset in Figure 1 shows the equivalent electrical circuit of the probe, with each electrical resistance serving both as a heater and thermometer. The probe is activated by an ultra-short pulse, with durations ranging from 100 ns to 200 µs and amplitudes between 1 V and 15 V. The thermal properties of the measured thin films are determined by examining the temperature increase in the metalized strips, patterned on the surface of the sample film, following a step change in input power (Joule heating). The measurement procedure involves analyzing the output voltage (ΔV), which depends on the change in electrical resistances due to temperature variations caused by Joule heating. In this measurement system, we employ the instruments depicted in Figure 1, using a precision-pulsed system for the input voltage (U). A precision digital oscilloscope measures the output voltage (ΔV) produced by a probe deposited on the material's surface to be characterized. This probe, consisting of a metallic strip directly deposited on the material under test, is intrinsically linked to the thermal properties of the material in contact. By configuring all bridge resistances on the same surface and with the same metal, we ensure uniform initial measurement conditions, such as temperature, pressure, and surface roughness. However, in this probe configuration, the self-balancing of the bridge is crucial to achieve good measurement sensitivity.

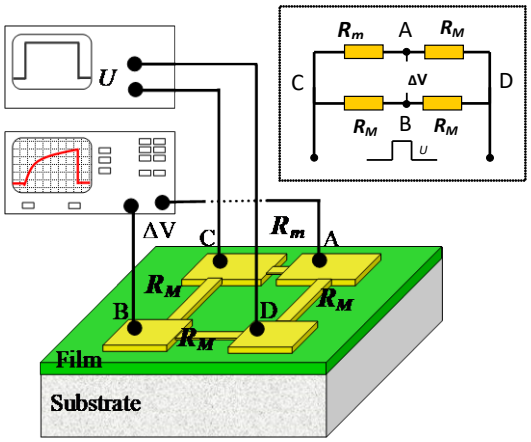

Fig. 1. Ultrafast THB technique for measuring the thermal properties of thin films. Experimental apparatus. A metal probe has 50 nm of thickness and patterned by photolithography on dielectric materials. The thermal properties of the sample film were determined by exploring the rate at which the temperature of the metal bridge increases with time subsequent to a step change of the input power (Joule heating). The temperature increase of the metal bridge was measured by detecting the output voltage ΔV resulting from a step change of the input voltage U. The inset demonstrates the equivalent electrical circuit of Ultra-fast THB technique.

To ensure self-balancing in our configuration, we have selected an identical ratio of length to width, set at 10, for each strip. Additionally, the proposed probes feature two types of electrical resistances: one of a larger size (referred to as macro-strip) and one of a smaller size (referred to as micro-strip), with the area ratio between the micro-strip and the macro-strip being 100 to 1. This specific ratio is chosen to concentrate the heating effect on the micro-strip, ensuring minimal heating on the macro-strip (area of micro-strip / area of macro-strip = 1 / 100). Consequently, the thermal transport properties of the thin films are determined by monitoring the variation in output voltage between pads A and B following a short pulse (ranging from 100 ns to 100 µs) applied between pads C and D (input voltage).

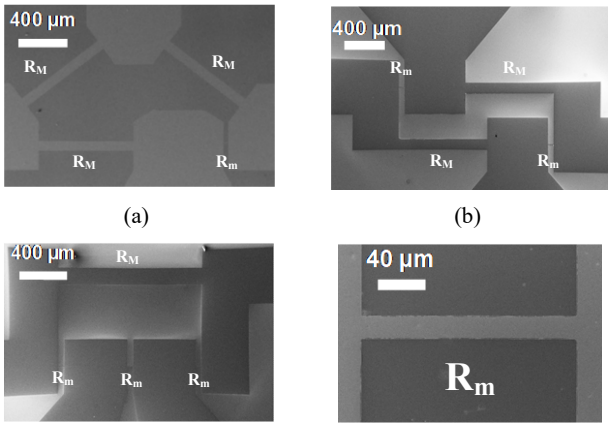

Fig. 2. Top view scanning electron microscope (SEM) images of the different types of probes, configured in Wheatstone bridge. (a) with one micro-strip, (b) with two micro-strips, (c) with three micro-strips, and (d) zoom on the micro-strip.

Three types of probes were developed. Figure 2 displays the top-view scanning electron microscopy (SEM) images of the three probes fabricated on SiO_2. The SEM images reveal that the probes consist of a very thin gold layer (approximately 50 nm) that

serves as a heater/thermometer. This layer was patterned using photolithography and lift-off processes on the sample, as illustrated in Figure 2. The gold layer was deposited at room temperature through DC magnetron sputtering from a pure gold target in argon plasma. This deposition technique was chosen to achieve a dense metallic film with excellent adhesion to the sample film. The thickness of the probes was calibrated to achieve a resistance of 50 Ohms and varies from 40 to 80 nm, depending on the deposition conditions and film roughness. We differentiated the three probes by the number of micro-strips. For instance, Figures 2(a), 2(b), and 2(c) depict probes with one, two, and three micro-strips, respectively. Figure 2(d) demonstrates that the micro-strip is well-defined and exhibits the expected dimensions.

The temperature variation ($\Delta T = T - T_0$) of the probe was determined by measuring the changes in output voltage, $\Delta V(t)$, which resulted from variations in resistance values. The electrical resistance of the micro-strip (R_m) and macro-strip (R_M) are related to temperature through the following relation:

$$\begin{cases} R_m = R_m^0\left(1+\beta(T_m - \mathrm{T}_0)\right) \\ R_M = R_M^0\left(1+\beta(T_M - \mathrm{T}_0)\right) \end{cases} \qquad (1)$$

with β and R_X^0 are respectively, the temperature coefficient and the electrical resistance at the initial temperature (T_0). The temperature coefficient resistance (β) is described as the sensitivity of the electrical resistance to temperature, and it is identified experimentally by measuring the probe resistance versus the temperature of the sample in a stationary regime. According to the metal thickness, β varied from 1.0 10^{-3} °C^{-1} to 2.5 10^{-3} °C $^{-1}$.

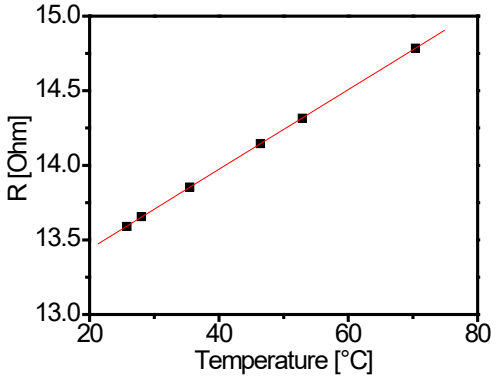

FIG. 3. Calibration of the probe. Probe resistance evolution with the temperature, patterned by magnetron sputtering at room temperature. The gold thickness was of 50 nm.

Figure 3 shows that the resistance change of the probe according to the temperature is linear between 20 °C and 80 °C. Therefore, one can deduce a temperature coefficient of 2 10^{-3} °C^{-1}. In practice, the temperature increase of the probe above the ambient did not exceed 80 °C. The output voltage (ΔV) can be written as a function of input voltage (U), with $R_m^0 = R_M^0$, for a probe with one micro-strip (see figure 2 (a)), as:

$$\Delta V = U\frac{\beta(\Delta T_m - \Delta T_M)}{2\left(2+\beta(\Delta T_m + \Delta T_M)\right)} \qquad (2)$$

This relationship can be simplified in the case of a small difference in temperature of the micro-strip (≈ 50 °C) and we neglect the heating of the macro-strip. The equation (2) becomes $\Delta V = \frac{U\beta\Delta T}{4}$. This simplification is also valid for the probe with three micro-strips (see figure 2 (c)). With two micro-strips (see figure 2 (b)), the ΔV of the probe can be written as:

$$\Delta V = U\frac{\beta(\Delta T_m - \Delta T_M)}{(2+\beta(\Delta T_m + \Delta T_M))} \approx \frac{U\beta\Delta T}{2} \qquad (3)$$

The relationship (3) shows that one can double the sensitivity to temperature measurement in the output voltage ($\frac{\partial(\Delta V)}{\partial(\Delta T)} = \frac{1}{2}U\beta$) in comparison to bridge with one micro-strip ($\frac{\partial(\Delta V)}{\partial(\Delta T)} = \frac{1}{4}U\beta$). Furthermore, the temperature (ΔT) was calculated hereafter by using a heat diffusion model based on the semi-analytical solution of the heat equation using an integral transform formulation.

Figure 4 provides an example of the input and output signals obtained at room temperature for SiO_2 with a thickness of 1200 nm, featuring a single micro-strip measuring 20 µm x 200 µm x 50 nm and three macro-strips measuring 200 µm x 2000 µm x 50nm. The heating pulse duration was 5 µs. The plots shown in Figure 4 indicate that the input voltage (U) was approximately 4 V, and the output voltage (ΔV) was around 100 mV. It can also be observed that the oscillations of the output signal were consistent with those of the input signal, indicating that the temperature and input power signals were convolved during this period.

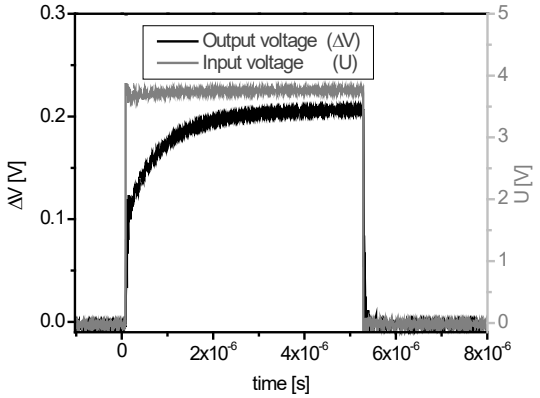

Fig. 4. Plots of the input voltage (continuous grid line) and the output voltage (continuous black line) of the probe versus time, measured for 5 µs time.

To circumvent the need for numerical treatment of the convolution process in estimating thermal properties, the time window for fitting was chosen to be between 100 ns and 5 µs. This selection ensured a constant input power within the specified time frame and established a direct correlation between temperature and input power, as outlined in relations (2) and (3). Should the electrical contact resistance with the terminal wires vary over time and temperature, then applying a current at varying rates would likely cause deviations in the signal. However, high reproducibility was observed, indicating that the electrical contact resistance did not significantly influence the results. This result was attributed to the fact that the contact resistances were significantly lower than the resistance of the strips. The thermal properties of the film were treated as free parameters, fitted to minimize the discrepancies between the model and the experimental signals. The fitting was carried out by minimizing a least squares function, following the approach reported in references [21] and [22]. The thermal properties were extracted by analyzing the output signal ΔV after measuring β and U, and using relations (2) or (3).

III. THEORETICAL SECTION

A. Electro-thermal simulations

The probe design was optimized through electro-thermal simulation using *Comsol Multiphysics* for finite element modeling (FEM). The design of the probe structures was developed to localize the heating within the micro-strip and to ensure uniform

power distribution along the heating strip. Additionally, it is crucial to minimize thermal interactions among all strips during the measurement time frame, which is less than 1 ms.

Furthermore, the bridge must be self-balanced at the initial temperature (T_0). In electro-thermal simulations, it is feasible to consider the complete structure of the probe—including all strips and contact pads—as well as the substrate material in contact. For the electrical analysis, we used a two-dimensional (2D) stationary potential model, justified by the metal's very thin thickness and the rapid diffusion process, which occurs on the order of nanoseconds. For the thermal analysis, a transient three-dimensional (3D) heat diffusion model was employed for the entire structure. These two aspects are interdependent: the input for the 3D heat diffusion model is the electrical power generated by Joule heating in the electrical model, which is used to calculate the temperature distribution. This calculated temperature, in turn, serves as an input parameter in the 2D electrical model to estimate the electrical conductivity, which is then used to estimate the electrical power. An example of an electro-thermal simulation is presented in Figures 5 and 6 for a probe featuring a single micro-strip. In this simulation, a metal probe with a thickness of 50 nm was patterned on a silicon substrate, having dimensions of 20 µm x 200 µm for the micro-strip, and 200 µm x 2000 µm for the macro-strips. One assumed that there is perfect contact between domains, and that losses within the structure were neglected. The distribution of electrical potential is depicted in Figure 5. We considered the input parameters to be 15 Ohms for the electrical resistance of each probe, 2 10^{-3} $°C^{-1}$ for the temperature coefficient, and 5 V for the input voltage with short pulses (refer to Figure 5). The power generated in each resistor of the probe is approximately 0.4 W.

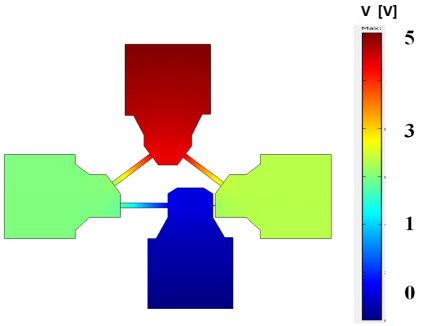

Fig. 5. Electro-thermal simulation result of electrical potential distribution for a probe with one micro-strip. The input voltage is 5 V.

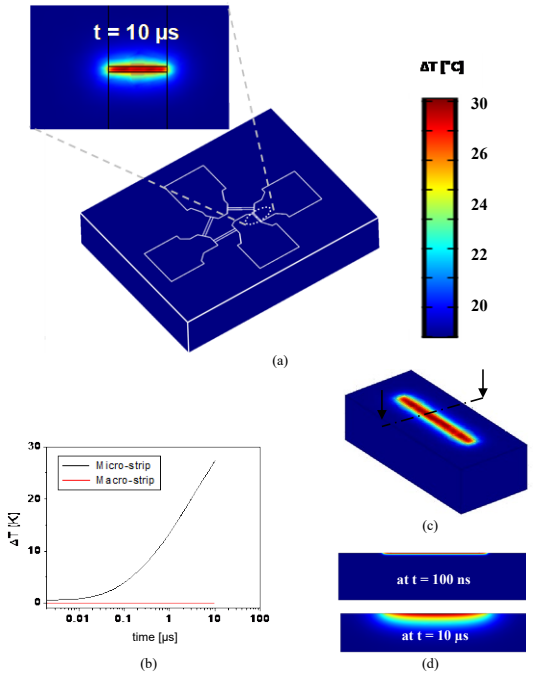

Fig. 6. Electro-thermal simulation result of temperature distribution (a) results with the tri-dimensional heat diffusion model on all the structure at t = 10 µs. The inset demonstrates a zoom of the heating of the micro-strip, (b) average temperature evolution versus time of the micro-strip and of the macro-strip, on silicon substrate. (c) results with the tri-dimensional heat diffusion model at t = 10 µs on the micro-strip and (d) cross section at 100 ns and at 10 µs with power of 0.4 W in each strip.

The resulting temperature distribution is illustrated in Figure 6(a), showing significant heating localized along the micro-strip compared to the rest of the structure (see inset of Figure 6(a)). The simulation results indicate that the average temperature of the micro-strips is higher than that of the macro-strip. This finding is depicted in Figure 6(b) as a function of time. As expected, the temperature of the micro-strip remains higher than that of the macro-strip across the entire measurement time range, contributing to more than 98 % of the resulting output voltage of the probe (refer to Figure 6(b)). The electro-thermal simulation requires considerable time and encounters difficulties when applied to complex structures due to meshing issues for both the probe and the thin layers. For this reason, at the initial stage, it is possible to simplify the correlation in electro-thermal simulation by separating the electrical potential model from the heat diffusion model. This approach is feasible owing to the homogeneous distribution of power along the metal strips (especially in the micro-strip) and the very low thickness of the probe (approximately 50 nm). Consequently, the simplified structure is depicted in Figure 6(c). A heat diffusion model is then constructed for a structure consisting of a micro-strip deposited on a sample. Figure 6(d) illustrates a cross-sectional view of the simplified structure at 100 ns and 10 µs, showing that the depth of heating increases gradually over the analysis time. This allows for the analysis of thicknesses ranging from a few nanometers to a few micrometers, depending on the time scale (refer to Figure 6(d)).

B. Heat diffusion model

The temperature evolution was theoretically determined as a function of thermal transport properties of the material layers, using a three-dimensional heat diffusion model. A calculation procedure was implemented for a structure comprising two layers, equivalent to a thin film deposited on a substrate, as depicted in Figure 7. The micro-strip acted as a rectangular heat source with negligible thermal mass, generating a constant power density. Due to the metal's thinness relative to the film thickness, the thermal

capacitance of the micro-strip was considered negligible. The transient temperature of the micro-strip was calculated by solving the three-dimensional heat diffusion equation in rectangular coordinates for each layer. The micro-strip has a length y_0 and a width x_0 deposited on the surface of the sample of length Ly and width Lx. In the heat diffusion model, according to reference,[23] we can obtain a linear relationship in Laplace transform domain between temperature ($\overline{\Delta T}$) and power density ($\overline{\varphi} = \frac{Q}{s\, x_0 y_0}$, Q is the power heat generated by the micro-strip, and s is Laplace variable). Such relationship is obtained by solving the 3D heat diffusion equation in the whole structure, as:

$$\overline{\Delta T}(s) = \overline{Z}(s)\ \overline{\varphi}(s) \qquad (4)$$

Where $\overline{Z}(s)$ is the thermal impedance of the sample in Laplace transform domain that depends on the thermal properties and the sample geometry. After calculating the averaged temperature and applying the Laplace transform and Finite Cosine Fourier transform, one can express the thermal impedance by formula (5):

$$\overline{Z} = \frac{1}{L_y}\frac{1}{L_x}\left\{\overline{\overline{Z}}_{0,0} + 2\sum_{n=1}^{N}\left[\frac{\sin\left(n\pi\frac{y_0}{L_y}\right)}{n\pi\frac{y_0}{L_y}}\right]^2\overline{\overline{Z}}_{0,n} + 2\sum_{m=1}^{M}\left[\frac{\sin\left(m\pi\frac{x_0}{L_x}\right)}{m\pi\frac{x_0}{L_x}}\right]^2\overline{\overline{Z}}_{m,0} + 4\sum_{n=1}^{N}\sum_{m=1}^{M}\left[\frac{\sin\left(n\pi\frac{y_0}{L_y}\right)}{n\pi\frac{y_0}{L_y}}\right]^2\left[\frac{\sin\left(m\pi\frac{x_0}{L_x}\right)}{m\pi\frac{x_0}{L_x}}\right]^2\overline{\overline{Z}}_{m,n}\right\} \qquad (5)$$

For a thin film attached to a semi-infinite substrate, the thermal impedance in Fourier-Laplace domain $\overline{\overline{Z}}_{m,n}$ is given by the relationship (6):

$$\overline{\overline{Z}}_{m,n} = \frac{1 + \frac{\gamma^s_{m,n} k_s}{\gamma^f_{m,n} k_f}\tanh(\gamma^f_{m,n} e_f)}{\gamma^s_{m,n} k_s + \gamma^f_{m,n} k_f \tanh(\gamma^f_{m,n} e_f)} \qquad (6)$$

And, $\gamma_{m,n} = \sqrt{\left(\frac{n\pi}{L_y}\right)^2 + \left(\frac{m\pi}{L_x}\right)^2 + \frac{\rho c\ s}{k}}$

where ρc, k and e are the heat capacity, effective thermal conductivity and thickness. Subscript f and S refer to the film and the substrate, respectively. ΔT in the time domain was obtained after inverse Laplace transformation using the *Gaver–Stehfest* algorithm.[24]

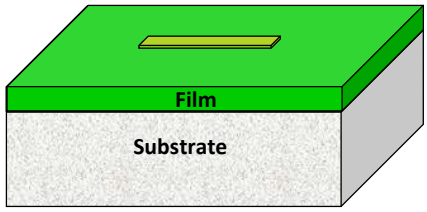

Fig. 7. Structure of the sample for the heat diffusion model associated with the ultrafast THB technique for measuring the thermal properties of thin films. The all metal strips are considered as a rectangular heat source of negligible thermal mass generating a constant power Q. All boundaries are insulated except for the bottom side of the substrate where a prescribed temperature is considered initial temperature.

IV. RESULTS AND DISCUSSION

The efficacy of the ultrafast THB (Transient Hot-Bridge) technique in measuring thermal properties at various initial temperatures is demonstrated through experiments. The THB measurements were carried out on amorphous SiO_2 thin films with a thickness of 1200 nm, deposited on a silicon substrate via thermal oxidation. As detailed in the experimental section, a gold probe featuring a single micro-strip (20 µm x 200 µm) and three macro-strips (200 µm x 2000 µm) was deposited on a SiO_2/Si sample measuring 10 mm x 10 mm x 500 µm. All thermal property fits discussed herein were derived from the output signals (ΔV), as previously defined.

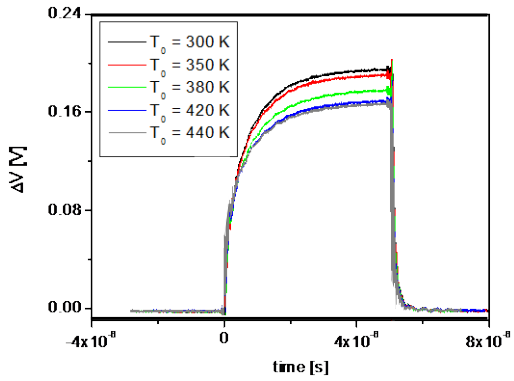

Fig. 8. Measured output signal ΔV of the probe with one micro-strip deposited on SiO_2 for different temperatures. All measurements are performed with the same input voltage. The pulse width is about 5 µs.

Measurements were reproducible, with replicate measurements yielding nearly identical thermal properties, indicating that the probe remained balanced under these conditions. The probe was placed in an oven with a temperature range between 300 K and 440 K. The output signals obtained at different temperatures are depicted in Figure 8. The observed decrease in the amplitude of the probe's output signal reflects the dependence of the SiO_2 film's thermal properties on the oven temperature. This decrease in amplitude is attributed to an increase in thermal conductivity within this temperature range. For each temperature setting, the thermal conductivity and heat capacity of SiO_2 were measured simultaneously. Figure 9(a) presents an example of the output voltage and fitted signals obtained at room temperature. In this figure, the measured and fitted signals are plotted in black and red continuous lines, respectively. The insets of Figure 9(a) indicate that the relative difference between the measured and the calculated temperatures did not exceed 4%. Such a fit is obtained by minimizing the objective function between the experimental signal and the mathematical model, by varying simultaneously the value of thermal conductivity, k, and heat capacity, ρc for 1200 nm-SiO_2. Finally the estimated values were found equal to 1.3 $Wm^{-1}K^{-1}$ for k, and 1.6 10^6 JKm^{-3} for ρc.

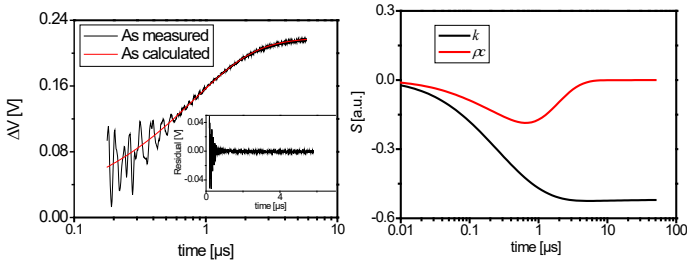

(a) (b)

Fig. 9. Results of an ultrafast THB measurement performed at room temperature on 1.2 µm of SiO_2 thermally grown on silicon. (a) Output voltage of the bridge versus time measured and predicted in the time window [0.1–5 µs]. (b) Evolution of the sensitivity coefficients for the measurement between 0.01 and 100 µs. The sensitivity coefficient S_k referring to the effective thermal

conductivity is plotted as a continuous red line. The sensitivity coefficient $S_{\rho c}$ referring to the volumic heat capacity is plotted as a continuous blue line.

Furthermore, figure 9 (b) gives the sensitivity coefficient of the thermal conductivity ($S_k = (k/T_{max})(\partial T/\partial k)$) and the heat capacity ($S_{\rho c} = (k/T_{max})(\partial T/\partial \rho c)$) of the SiO_2 film with respect to the temperature T are plotted respectively, in continuous black, and red lines in the range time [0.01 µs and 100 µs]. The sensitivity curves reveal that we can extract simultaneously the thermal conductivity and heat capacity with a high precision for SiO_2 film. In practice, parameter estimation is performed in the time interval 0.1-1 µs for ρc and 1-5 µs for k because we have a maximum sensitivity in this time range, and these two thermal properties are not correlated. These values are in good agreement with the already published data. For example in reference [25], the thermal conductivity at room temperature was found equal to 1.34 $Wm^{-1}K^{-1}$ and in references [26] and [27], the reported heat capacity also at room temperature was equal to 1.59 10^6 J Km^{-3}. Moreover, we measured the thermal properties for other initial temperatures than 300 K, the results are shown in figures 10 (a) and 10 (b).

Figures 10 (a) and 10 (b) show estimations of the thermal conductivity k and the specific heat, *c*, between 300 K and 440 K, respectively. The specific heat is obtained from the heat capacity experimentally measured and volume density $\left(c = (\rho c)/\rho\right)$, given in reference [27] and supposed constant with the temperature. The thermal conductivity and heat capacity values are obtained simultaneously by the analysis of each signal, shown in Figure 10 (a). The values obtained in this temperature range are in good agreement with the values reported in the literature for both the thermal conductivity [25] and specific heat [26]. Moreover, the performances of the THB technique was employed in order to measure the thermal conductivity of materials with high thermal dissipation, such as sapphire substrate and aluminum nitride (*AlN*) thin-film.

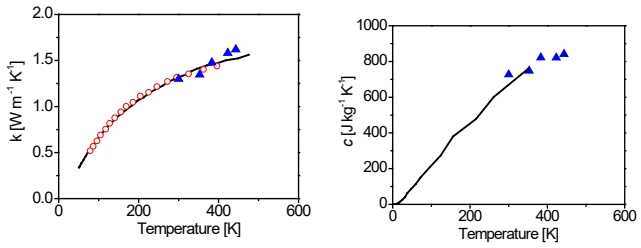

(a) (b)

Fig. 10. Thermal properties measured as a function of the initial temperature for 1200 nm-SiO_2 on Si substrate, (a) *k* versus temperature: with blue solid triangles our measurements, with circle voids data given in reference 24, and with a continuous black line the bulk SiO_2 [24]. (b) *c* versus temperature with blue solid triangles our measurements and with continuous black line the bulk SiO_2 values [26].

Sapphire Substrate – Figure 11 gives the output voltage (ΔV) measured between 100 ns and 20 µs in the case of micro-strip patterned on sapphire substrate. In figure 11, the measured signal is plotted in black line with the fitted signal in red line given for a substrate thermal conductivity of 43 $W.m^{-1}.K^{-1}$. The heat capacity of sapphire was taken equal to 3.2 10^6 $J.m^{-3}.K^{-1}$ [28]. The insert of figure 11 indicates a difference between the signals down to 2 % on the overall time-window [100 ns, 20 µs]. This explains the good agreement which was found between the measured signal and the calculated model. The uncertainty on the thermal conductivity of sapphire was estimated to ± 5 $W.m^{-1}.K^{-1}$. The extracted value was very close to the literature value for sapphire given in references [28] and [29]. All tests performed on sapphire revealed the good performance of the technique and ability of the measurement system for determining precisely the thermal conductivity of substrate materials.

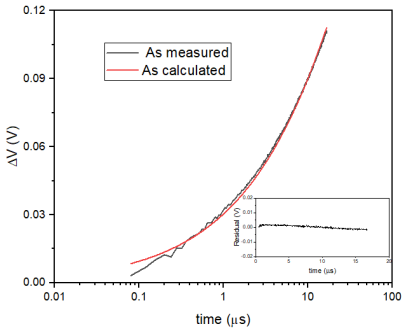

Fig. 11. Results of a THB measurement performed at room temperature on sapphire substrate.

AlN thin-film – AlN films are intensively explored as potential materials for applications in high-temperature microelectronic devices [30, 31]. The thermal conductivity of bulk AlN single crystals can be as high as 320 $W.m^{-1}.K^{-1}$ [30]. We have measured the thermal conductivity of crystallized AlN thin films, which were deposited by reactive magnetron sputtering from a pure Al target in a nitrogen-argon plasma [31]. Magnetron sputtering is recognized as a versatile deposition technique for producing dense and highly textured films with a large grain size and low oxygen content [31]. The results of the fits presented in Figure 12 were obtained on AlN films 3.5 µm thick, deposited on a layered substrate. This substrate consists of a single-crystal silicon (100) substrate coated with a sputtered silicon nitride (SiN) film 250 nm thick. Figure 12 presents the time- ΔV signals measured on the AlN films over the time windows [0.1 µs - 100 µs]. The heat capacity of the AlN films was assumed to be equal to the bulk value of 2.7 10^6 $J.m^{-3}.K^{-1}$ [32]. The effective thermal conductivity of the SiN film was also determined using our technique [23], with an obtained value of 0.70 $W.m^{-1}.K^{-1}$, which is in good agreement with other experimental data [33,34]. Consequently, the effective thermal conductivity of the films deposited on silicon and silicon nitride substrates was found to be 125 $W.m^{-1}.K^{-1}$. The insets of Figure 12 indicate that the difference between the measured and the calculated signal did not exceed 2 %. It is evident that the measured thermal conductivity values are effective as they consider not only the film itself but also the AlN/SiN interfacial thermal resistance.

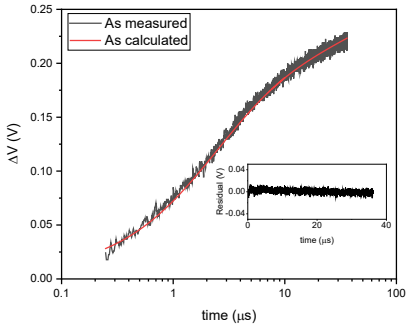

Fig. 12. Results of a THB measurement performed at room temperature on 3.5 µm of aluminium nitride deposited by magnetron sputtering on 250nm-SiN/silicon (100) substrate.

V. Conclusion

The Ultrafast Transient Hot-Bridge technique has been successfully implemented for measuring the thermal properties of thin films. Precise measurements of these properties were conducted using an experimental setup that generates ultra-short electrical pulses, enabling the probing of subsequent temperature increases on both nanosecond and microsecond timescales. A novel probe structure was developed specifically for the measurement of thin films thermal properties. These probes, fabricated from resistive

metal strips, are configured into a Wheatstone bridge circuit, with the design optimized to achieve a linear relationship between the output voltage and the micro-strip temperature. Experiments were performed on amorphous SiO_2 deposited on silicon substrates at various initial temperatures, demonstrating the technique's capability to precisely measure the thermal properties of thin films under any initial measurement conditions. Developed to accommodate a wide range of materials—from those with low to very high conductivity—this technique has been applied to AlN thin films, which are known for their higher conductivity, yielding an effective thermal conductivity value of 125 $Wm^{-1}K^{-1}$. These measurements not only underscore the versatility of our technique but also highlight its potential to extract the effective thermal conductivity of a layer atop a stacked layer, provided the thermal conductivity of each underlying layer is known.

ACKNOWLEDGEMENTS

Nantes Université financial help is appreciated for supporting this work within the framework of the Program “AAP "Mission Invité 2023" (*Vague exceptionnelle*)”. This work is dedicated to Professor *Y. Scudeller* who passed away not long ago, and without his previous works, this one could not be achieved.

REFERENCES

[1] B. E. Belkerk, A. Soussou, M. Carette, M. A. Djouadi, and Y. Scudeller, “Structural-dependent thermal conductivity of aluminium nitride produced by reactive direct current magnetron sputtering,” Applied Physics Letters, vol. 101, no. 15, p. 151908, Oct. 2012, doi: https://doi.org/10.1063/1.4757298.

[2] B. E. Belkerk et al., “Substrate-dependent thermal conductivity of aluminum nitride thin-films processed at low temperature,” Applied physics letters, vol. 105, no. 22, Dec. 2014, doi: https://doi.org/10.1063/1.4903220.

[3] S. A. Govorkov, W. Ruderman, M. W. Horn, R. B. Goodman, and M. Rothschild, “A new method for measuring thermal conductivity of thin films,” Review of Scientific Instruments, vol. 68, no. 10, pp. 3828–3834, Oct. 1997, doi: https://doi.org/10.1063/1.1148035.

[4] J. Yang, J. Zhang, H. Zhang, and Y. Zhu, “Thermal conductivity measurement of thin films by a dc method,” Review of scientific instruments online/Review of scientific instruments, vol. 81, no. 11, Nov. 2010, doi: https://doi.org/10.1063/1.3481787.

[5] N. Stojanovic, J.-H. Yun, E. B. K. Washington, J. M. Berg, M. Holtz, and H. Temkin, “Thin-Film Thermal Conductivity Measurement Using Microelectrothermal Test Structures and Finite-Element-Model-Based Data Analysis,” vol. 16, no. 5, pp. 1269–1275, Oct. 2007, doi: https://doi.org/10.1109/jmems.2007.900877.

[6] D. G. Cahill, “Thermal conductivity measurement from 30 to 750 K: the 3ω method,” Review of Scientific Instruments, vol. 61, no. 2, pp. 802–808, Feb. 1990, doi: https://doi.org/10.1063/1.1141498.

[7] M.-J. Huang, T.-Y. Chang, H.-C. Chien, W.-C. Sun, and D.-J. Yao, “The Thickness Difference Method for Measuring the Thermal Conductivity of Thick Films,” Journal of microelectromechanical systems, vol. 19, no. 4, pp. 895–902, Aug. 2010, doi: https://doi.org/10.1109/jmems.2010.2051534.

[8] Z.-X. Zong, Z.-J. Qiu, S.-L. Zhang, Reinhard Streiter, and R. Liu, “A generalized 3ω method for extraction of thermal conductivity in thin films,” Journal of applied physics, vol. 109, no. 6, Mar. 2011, doi: https://doi.org/10.1063/1.3559299.

[9] C. A. Paddock and G. L. Eesley, “Transient thermoreflectance from thin metal films,” Journal of applied physics, vol. 60, no. 1, pp. 285–290, Jul. 1986, doi: https://doi.org/10.1063/1.337642.

[10] P. L. Komarov, M. G. Burzo, Gunhan Kaytaz, and P. E. Raad, “Transient thermo-reflectance measurements of the thermal conductivity and interface resistance of metallized natural and isotopically-pure silicon,” Microelectronics, vol. 34, no. 12, pp. 1115–1118, Dec. 2003, doi: https://doi.org/10.1016/s0026-2692(03)00201-5.

[11] Naoyuki Taketoshi, T. Baba, and A. Ono, “Development of a thermal diffusivity measurement system for metal thin films using a picosecond thermoreflectance technique,” Measurement Science and Technology, vol. 12, no. 12, pp. 2064–2073, Nov. 2001, doi: https://doi.org/10.1088/0957-0233/12/12/306.

[12] A. Jain and K. E. Goodson, “Measurement of the Thermal Conductivity and Heat Capacity of Freestanding Shape Memory Thin Films Using the 3ω Method,” Journal of Heat Transfer, vol. 130, no. 10, Aug. 2008, doi: https://doi.org/10.1115/1.2945904.

[13] R. Fleeter, J. Kestin, and W. A. Wakeham, “The thermal conductivity of three polyatomic gases and air at 27.5°C and pressures up to 36 MPa,” Physica. A, vol. 103, no. 3, pp. 521–542, Oct. 1980, doi: https://doi.org/10.1016/0378-4371(80)90023-0.

[14] S. E. Gustafsson, E. Karawacki, and M. N. Khan, “Determination of the thermal-conductivity tensor and the heat capacity of insulating solids with the transient hot-strip method,” Journal of Applied Physics, vol. 52, no. 4, pp. 2596–2600, Apr. 1981, doi: https://doi.org/10.1063/1.329068.

[15] S. Ohkubo and M. Okuda, “A method for the determination of the thermal transport properties of submicron-thick dielectric films with the use of an analytical expression,” Thin Solid Films, vol. 219, no. 1–2, pp. 239–243, Oct. 1992, doi: https://doi.org/10.1016/0040-6090(92)90751-v.

[16] M. Okuda and S. Ohkubo, “A novel method for measuring the thermal conductivity of submicrometre thick dielectric films,” Thin Solid Films, vol. 213, no. 2, pp. 176–181, Jun. 1992, doi: https://doi.org/10.1016/0040-6090(92)90280-o.

[17] S. E. Gustafsson and E. Karawacki, “Transient hot-strip probe for measuring thermal properties of insulating solids and liquids,” Review of Scientific Instruments, vol. 54, no. 6, pp. 744–747, Jun. 1983, doi: https://doi.org/10.1063/1.1137466.

[18] G. Velve Casquillas, M. Le Berre, C. Peroz, Y. Chen, and J. J. Greffet, “Microlitre hot strip devices for thermal characterization of nanofluids,” Microelectronic engineering, vol. 84, no. 5–8, pp. 1194–1197, May 2007, doi: https://doi.org/10.1016/j.mee.2007.01.187.

[19] U. Hammerschmidt and V. Meier, “New Transient Hot-Bridge Sensor to Measure Thermal Conductivity, Thermal Diffusivity, and Volumetric Specific Heat,” International Journal of Thermophysics, vol. 27, no. 3, pp. 840–865, May 2006, doi: https://doi.org/10.1007/s10765-006-0061-2.

[20] R. Model, R. Stosch, and U. Hammerschmidt, “Virtual Experiment Design for the Transient Hot-Bridge Sensor,” International Journal of Thermophysics, vol. 28, no. 5, pp. 1447–1460, Feb. 2007, doi: https://doi.org/10.1007/s10765-007-0152-8.

[21] Stéphane Orain, Yves Scudeller, and Thierry Brousse, “Thermal conductivity of ZrO thin films,” International journal of thermal sciences, vol. 39, no. 4, pp. 537–543, Apr. 2000, doi: https://doi.org/10.1016/s1290-0729(00)00234-9.

[22] S. Orain, Y. Scudeller, S. Garcia, and T. Brousse, “Use of genetic algorithms for the simultaneous estimation of thin films thermal conductivity and contact resistances,” International Journal of Heat and Mass Transfer, vol. 44, no. 20, pp. 3973–3984, Oct. 2001, doi: https://doi.org/10.1016/s0017-9310(01)00025-4.

[23] B. E. Belkerk, M. A. Soussou, M. Carette, M. A. Djouadi, and Y. Scudeller, “Measuring thermal conductivity of thin films and coatings with the ultra-fast transient hot-strip technique,” Journal of Physics D: Applied Physics, vol. 45, no. 29, p. 295303, Jul. 2012, doi: https://doi.org/10.1088/0022-3727/45/29/295303.

[24] H. Stehfest, “Remarks on algorithm 368, Numerical inversion of Laplace transforms”, Comm. A.C.M. (1970), n°13, 624.

[25] D. G. Cahill and T. H. Allen, “Thermal conductivity of sputtered and evaporated SiO2 and TiO2 optical coatings,” Applied Physics Letters, vol. 65, no. 3, pp. 309–311, Jul. 1994, doi: https://doi.org/10.1063/1.112355.

[26] R. C. Zeller and R. O. Pohl, “Thermal Conductivity and Specific Heat of Noncrystalline Solids,” Physical Review B, vol. 4, no. 6, pp. 2029–2041, Sep. 1971, doi: https://doi.org/10.1103/physrevb.4.2029.

[27] S.-M. . Lee and D. G. Cahill, “Heat transport in thin dielectric films,” Journal of Applied Physics, vol. 81, no. 6, pp. 2590–2595, Mar. 1997, doi: https://doi.org/10.1063/1.363923.

[28]T. Reddyhoff, A. Schmidt, and H. Spikes, “Thermal Conductivity and Flash Temperature,” Tribology Letters, vol. 67, no. 1, Jan. 2019, doi: https://doi.org/10.1007/s11249-018-1133-8.

[29] D. G. Cahill, S.-M. . Lee, and T. I. Selinder, “Thermal conductivity of κ-Al2O3 and α-Al2O3 wear-resistant coatings,” Journal of Applied Physics, vol. 83, no. 11, pp. 5783–5786, Jun. 1998, doi: https://doi.org/10.1063/1.367500.

[30] C. Duquenne et al., “Magnetron Sputtering of Aluminium Nitride Thin Films for Thermal Management,” Plasma processes and polymers, vol. 4, no. S1, pp. S1–S5, Apr. 2007, doi: https://doi.org/10.1002/ppap.200730101.

[31] C. Duquenne, M-P. Besland, P. Y. Tessier, E. Gautron, Y. Scudeller, and D. Averty, “Thermal conductivity of aluminium nitride thin films prepared by reactive magnetron sputtering,” Journal of Physics D: Applied Physics, vol. 45, no. 1, p. 015301, Dec. 2011, doi: https://doi.org/10.1088/0022-3727/45/1/015301.

[32] LI Berger, Semiconductor Materials, CRC Press, 1997, ISBN 0-8493-8912-7

[33] S.-M. . Lee and D. G. Cahill, “Heat transport in thin dielectric films,” Journal of Applied Physics, vol. 81, no. 6, pp. 2590–2595, Mar. 1997, doi: https://doi.org/10.1063/1.363923.

[34] B. E. Belkerk, J. Camus, B. Garnier, H. Al Brithen, S. Sahli, and M.-A. . Djouadi, “Measuring anisotropic thermal conductivity of aluminum nitride films with the ultra-fast hot strip technique,” International Journal of Thermal Sciences, vol. 151, p. 106259, May 2020, doi: https://doi.org/10.1016/j.ijthermalsci.2019.106259.